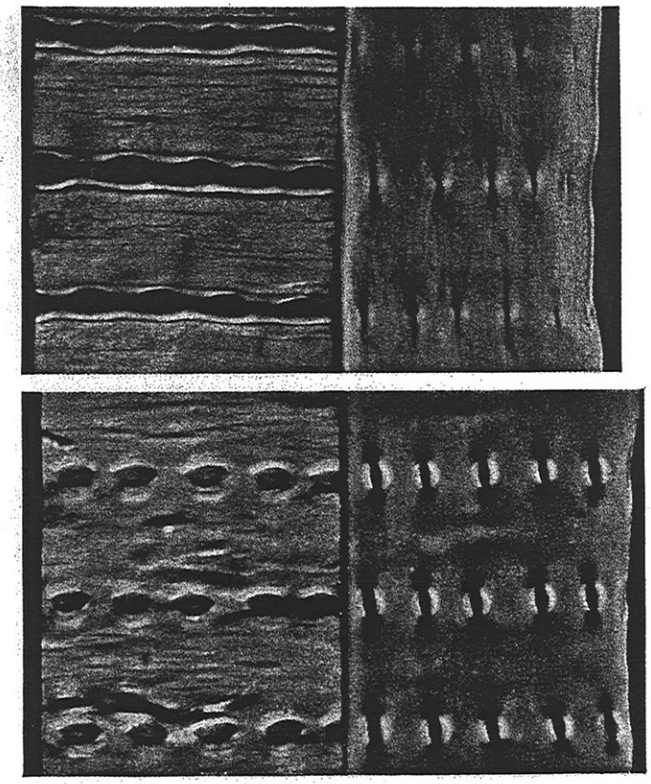

Fig. 9.1 Polarization photomicrographs with a Red I plate of the outer (left) and inner (right) wall layer of the central siphon of some Dasycladaceae. For explanation, see text.

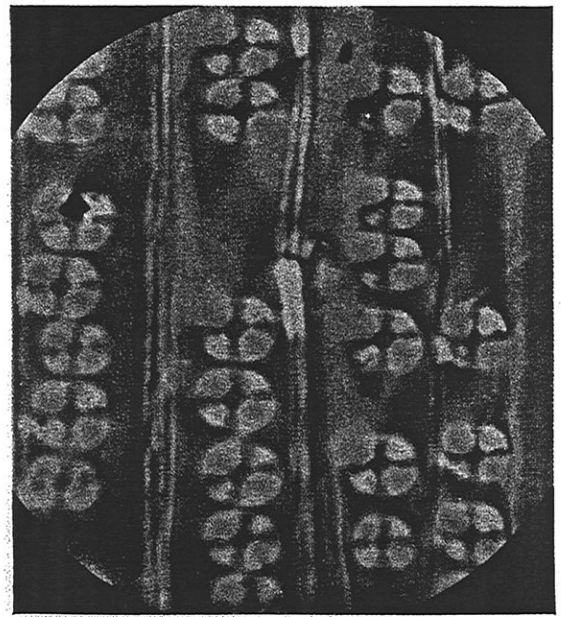

Fig. 10.16 The appearance of bordered pits in conifer

The Physical Biology of Plant Cell Walls

R. D. Preston F.R.S.

Professor Emeritus and former Head of Astbury Department of Biophysics, University of Leeds

London

Chapman and Hall

First published 1974
by Chapman and Hall Ltd.
11 New Fetter Lane, London ECP 4EE

Set by EWC Wilkins Ltd, London N12 0EH
and printed in Great Britain by Fletcher & Son Ltd, Norwich

ISBN 0 412 11600 6

Distributed in the U.S.A.
by Halsted Press, a Division
of John Wiley & Sons, Inc., New York

Library of Congress Catalog Card Number 73/21335

To Eva, my wife and colleague

CHAPTER 4

Structure determination – optical microscopy

4.1 The principles of microscopy

These various chemical constituents form a complex assembly in the wall which can be examined by a number of physical methods. Since there is always present at least one polysaccharide which is crystalline, methods designed for the elucidation of crystal structure are particularly suitable and the next two chapters will be devoted to two of the more powerful methods falling in this category. It should be noted that although the general structure of many walls has now been worked out by these methods an understanding of the techniques themselves remains important. The structure of walls is very variable, so that in investigating any particular piece of wall in hand the structure has often to be re-worked just as though nothing were yet known about it. We begin with techniques of microscopy.

Any study of a cell wall as of any other biological entity demands that the material should be examined at all possible levels of size. Observation by eye alone is of limited value, chiefly on account of the low resolving power of the eye, i.e. the relatively large separation between points in the object which can still be seen as two points as the points are moved closer together. An object can be focussed on the retina provided that the intervening distance is greater than a critical value known as the closest distance of distinct vision, about 250 mm with a normal eye. At this distance the resolving power is 0.2 mm and detail smaller than this cannot be seen. This is why most cell walls presented edgewise to the eye are invisible. Visualization is achieved by interposing between the object and the eye an optical system in such a way that

the object is so magnified that detail smaller than 0.2 mm becomes at least this size, and the system must be such that its own resolving power is better than 0.2 mm. The system is, of course, a microscope. There is nowadays, a battery of microscopes available to the cytologist; these all have principles in common and these will be described first. The complications involved with the various microscope types will then be taken up in so far as necessary for the rest of the book.

It should be clear that the fundamentally important attribute of any microscope is its resolving power r. Clearly it is formally desirable only that a microscope should magnify an object to the extent that a distance r in the object should become 0.2 mm in the image; for then all the detail resolvable by the microscope is also resolvable by the eye. The useful magnification is therefore $0.2/r$ where r is in mm and, though greater magnification than this may be used for comfort of viewing, nothing further is gained. In light microscopy, simple lenses suffer from aberrations which materially reduce the resolving power below that theoretically attainable which will be derived below. For this reason microscope lenses are complex, consisting of trains of lenses, some of which are closely in contact and some of which are spaced. The reasons for such complexity will not be discussed further here; interested readers are referred to texts on microscopy. Lenses will be dealt with as though they were simple biconvex lenses.

Before considering the resolving power of a microscope we need to be reminded of some simple considerations concerning the nature of light and other electromagnetic radiations.

4.2 The wave nature of electromagnetic radiation

A beam of light passing through a homogeneous medium is associated with an electric vector and a magnetic vector, the magnitudes of which fluctuate at any point between limits, the end of the vector moving in simple harmonic motion. We will consider only the electric vector. If the vibration is conceptually halted, the locus of the vector in space is as shown in Fig. 4.1a, namely a sine curve. This sine wave can be specified by two parameters, (a) the *wavelength*, λ, between identical points on the curve, (b) the frequency, ν, i.e. the number of crests, say, which pass a given point per second

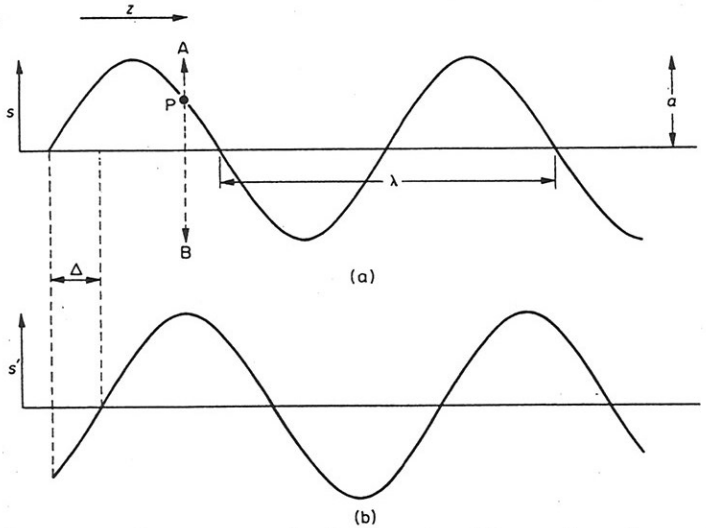

Fig. 4.1 Two sine waves, amplitude *a*, wavelength λ out of step by a path difference Δ.

when the vibration is again set in motion. Clearly the product $\nu\lambda$ equals the velocity of light, c. If the period is τ (i.e. the time for P (Fig. 4.1a) to pass from A to B and back to A) the wave vibration may be written as

$$s = a \sin 2\pi\left(\frac{t}{\tau} - \frac{z}{\lambda}\right) \qquad 4.1$$

A second vibration, passing from left to right parallel to the first and identical with it except that it is out of step by a distance Δ (Fig. 4.1b) may equally be written

$$s' = a \sin 2\pi\left[\left(\frac{t}{\tau} - \frac{z}{\lambda}\right) - \frac{\Delta}{\lambda}\right] \qquad 4.2$$

When $\Delta = \lambda$, this reduces to Equation 4.1 and the two vibrations reinforce each other. They are again in step. When $\Delta = \lambda/2$, on the other hand, the two vibrations are as far out of step as they can be, Equation 4.2 becomes

$$s' = -a \sin 2\pi\left(\frac{t}{\tau} - \frac{z}{\lambda}\right) = -s,$$

and at all points and all times the vibrations cancel. The intensity has become zero. This is destructive interference.

The path difference, Δ, may be considered in another way. Consider a point P, Fig. 4.2, moving uniformly along a circular path of radius a with angular velocity ω ($= 2\pi/\tau$). As P moves, the foot N of the perpendicular from P to the vertical diameter AB of the circle moves in such a way that

$$\text{ON} = s = a \sin\theta = a \sin\omega t \qquad 4.3$$

For a second point P′, an angular distance δ behind P, the corresponding motion along AB is

$$s' = a \sin(\omega t - \delta) \qquad 4.4$$

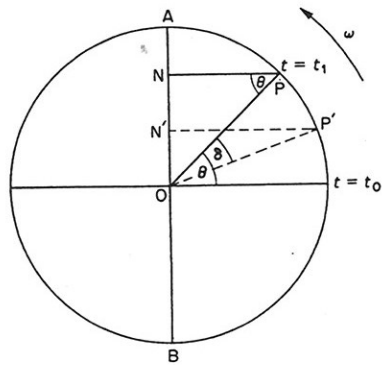

Fig. 4.2 For explanation, see text.

Comparison of Equation 4.3 with 4.2 (taking $z = 0$) shows that

$$\frac{2\pi\Delta}{\lambda} = \delta \qquad 4.5$$

The path difference Δ can therefore be expressed as a *phase difference* δ. When $\delta = 2\pi$ the two vibrations are in step; when $\delta = \pi$ they are out of step and destructive interference is complete. In considering microscopy in terms of the wave nature of light it is convenient to use Equation 4.4 in place of equations of the type of 4.2, with no loss of rigour.

4.3 Resolving power

The efficiency of an optical system may be judged by the accuracy

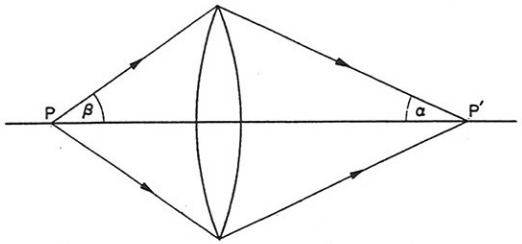

Fig. 4.3 A point object, P, producing a point image P′ through a lens system.

with which a mathematical point P on the object, Fig. 4.3, (taken on the optic axis for simplicity) is recorded as a mathematical point P′ on the image. Consider the space on the image side of the lens, the image space, and assume, as is usual in theories of microscopy, that the object P is self-luminous. Suppose further that the converging beam of light in image space is limited by a rectangular stop LMNO as in Fig. 4.4. Through F, the image position, draw a *very short* line FF′ (= h) parallel to the plane LMNO and to MN or OL. Then since the wave trains centering upon F are parts of spherical sheets whose centre if F, FF′ is part of a diameter of the spheres. We wish to enquire under what circumstances light of appreciable intensity will impinge upon F′, i.e. how 'blurred' the image F will be.

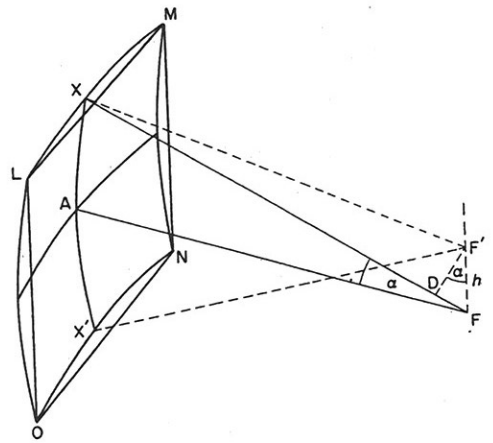

Fig. 4.4 For explanation, see text.

Since FF′ is a diameter, LM and ON are parallels of latitude and all points on each of them are equidistant from F′. Light vibrations passing from all points on LM will arrive at F′ in phase so that the phase from the whole strip may be taken as the phase from its mid-point X, and similarly for ON. The difference in phase between the light reaching F′ from LM and ON is therefore equivalent to the path difference X′F′ − XF′.

To evaluate this, note that if h is small, XF′ = XD and

$$XF - XF' = XF - XD = h \sin \alpha$$

Similarly, $$X'F' - X'F = h \sin \alpha$$

Since XF = X′F, this means that

$$X'F' - XF' = 2h \sin \alpha$$

$$\text{or } AF' - XF' = h \sin \alpha$$

Clearly when AF′ − XF′ = λ/2 for any narrow horizontal strip above A, there is another below it, contributing opposite phase. Therefore, for all the light passing through LMNO there will be zero intensity at F′ only when

$$h = \lambda/(2 \sin \alpha) \qquad 4.6$$

There will, on the other hand, be a maximum of intensity when

$$h = \lambda/\sin \alpha,$$

and additional minima at $3\lambda/(2 \sin \alpha)$, $5\lambda/(2 \sin \alpha)$, etc. and maxima at $2\lambda/\sin \alpha$, $3\lambda/\sin \alpha$, etc. Had a circular aperture been used, the calculation would have been more difficult, but the result would have been only to replace 1/2 in Equation 4.6 by 0.61; and if the whole operation had been carried out in a medium of refractive index n instead of *in vacuo*, as assumed, all distances would need to be multiplied by n [since this is the ratio of (velocity of light *in vacuo*)/(velocity of light in medium)]. The first minimum of intensity would then be at

$$h = \frac{0.61\lambda}{n \sin \alpha} \qquad 4.7$$

and this is the formulation we shall adopt.

The nature of light itself, therefore, however perfect are the lenses used, sets a limit of the accuracy with which an optical system can image a mathematical point. A point in the object

becomes in the image a disc surrounded by a series of concentric annular rings of decreasing intensity, the Airey disc (Fig. 4.5). A second point in the object close to the first will be reproduced as a second Airey disc in the image and there is clearly a limit beyond which these discs may approach each other and remain visually separate. This limit is taken as the point at which the centre of the central maximum of one disc lies squarely over the first minimum of the other, when the overall intensity distribution (Fig. 4.5) is virtually that of a single broader image.

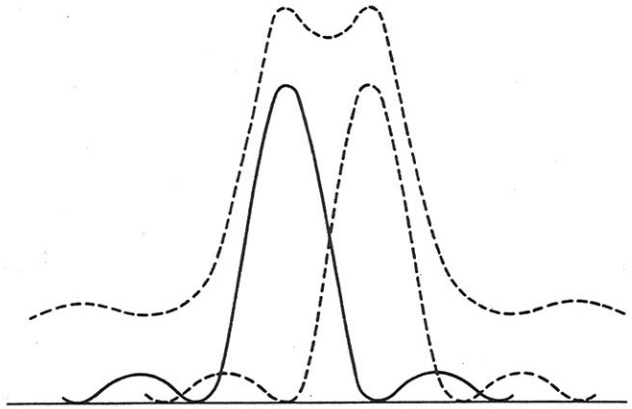

Fig. 4.5 Two overlapping Airey discs in image space, representing two close points in object space.

At this point the distance between the Airey discs is $(0.61)\lambda/n \sin \alpha$. The corresponding distance in object space (Fig. 4.3) is clearly $(0.61)\lambda/n \sin \beta$ and this is the resolving power of the optical system, r.

$$r = (0.61)\lambda/n \sin \beta.$$

This equation applies to all radiation and therefore also to the electron microscope. For visible light, remembering that β can at most be $\pi/2$ (and is of course in practice much less than this) so that the maximum value of $\sin \beta$ is 1, and taking $\lambda = 0.5\,\mu m$ (yellow light) and $n = 1.5$, then $r = 0.2\,\mu m$ and this is the limit below which no optical instrument can go. It follows that, since the resolving power of the eye is 0.2 mm, the maximum useful magnification of a system using yellow light is 0.2 mm/0.2 μm = 1000X.

The value of $n \sin \beta$ for the objective lens of a microscope (the lens which determines the actual resolving power) is called the numerical aperture, n.a., and is commonly marked on the lens (assuming use of the correct immersion oil in immersion objectives). In the critical use of a microscope it is always necessary to ensure that the n.a. of the objective is sufficiently high to resolve the detail required.

Other matters dealing with image formation are deferred until interference microscopy is discussed (p. 108).

4.4 The polarizing microscope

Just as the light microscope is still a very powerful tool in biology, so the polarizing microscope is still mandatory in all laboratories dealing with matter in the crystalline state, including biological tissues, organs or organelles which are crystalline. Under this microscope crystalline material can be recognized and the crystal axes determined even if the crystals are submicroscopic in size; and the nature of the crystalline material can often be defined. It is an ordinary light microscope built with certain precautions including devices to produce and detect *plane polarized light*.

When a ray of light passes through a crystal with symmetry less than cubic (e.g. orthorhombic, tetragonal or monoclinic) it is usually divided into two rays which travel through the crystal with different velocities and therefore different refractive indices (Fig. 4.6). Moreover, although the incident light vibrates in all directions at right angles to the direction of propagation, the refracted beams

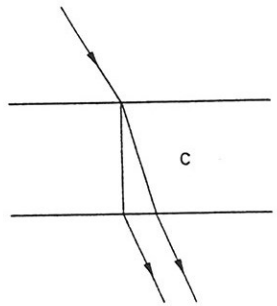

Fig. 4.6 Double refraction by a crystalline plate, C.

each vibrate in one direction only; and the vibrations occur in two planes at right angles to each other. The refracted beams are said to be plane polarized. If the incident beam falls normally on the face of the crystal, or otherwise if the crystal is thin enough, the two refracted beams overlap. Although they are statistically coherent since they are derived from the same beam, they do not interfere since the planes of vibration are at right angles. In all the material with which we shall deal, one vibration direction in the crystal always lies in the plane containing a crystal axis and the ray; the other, lying at right angles to this, also lies along a crystal axis in orthorhombic and tetragonal crystals. This forms the basis of the technique of polarization microscopy.

If one of the two beams is isolated (by deflecting the other away in a Nicol prism or by passing through a polaroid), the unique vibration direction of the other beam may be used as a probe to detect the axes in a second crystal.

Consider a hypothetical crystal consisting of a parallel array of diatomic molecules in which the atoms are joined by primary valences and the molecules are associated by secondary valences. Then the molecules lie further from each other than do the atoms in the molecule. Consider one of the atoms (Fig. 4.7). When a plane polarized beam passes through the crystal normal to the plane containing the primary valences and with the electric vector vibrating parallel to the direction of the bond (Fig. 4.7a), displacements within the atom separates negative from positive charges instantaneously as shown. The atoms are electrically polarized (using this term now in a different sense) and since the nearest neighbours are of opposite sign, the polarization is increased by induction. By the same token, when the electric vector lies at right angles to the

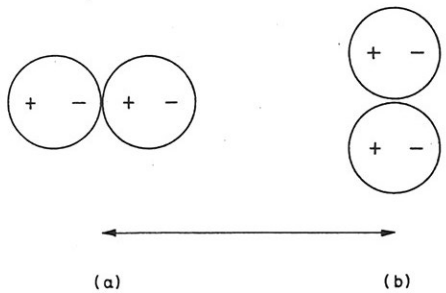

Fig. 4.7 For explanation, see text.

direction of the bond the polarization is reduced (Fig. 4.7b). The electric field in the visible region of the spectrum is changing its direction between 4 and 7.5×10^{14} times per second and only the electrons can respond to such rapid oscillations. We are therefore dealing here solely with polarization due to displacements of the electron atmosphere of the atoms.

Accepting the Lorenz-Lorenz equation connecting the refractive index n and the polarizability

$$\frac{n^2 - 1}{n^2 + 2} = k, \qquad k \text{ being constant for any one medium,}$$

it may be seen that a higher polarization is associated with a higher refractive index, and the crystal is optically *anisotropic*. The medium has the higher refractive index when the light is vibrating parallel to bond direction.

Transferring this concept to a real organic 'crystal' consisting of an assembly of parallel molecular chains, only the links within the chain being primary valences, then the allowed vibration directions within the crystal lie parallel and perpendicular to chain length; and the vibration direction lying parallel to chain length has the higher refractive index. Both the chain direction and the refractive indices can then be determined. We consider first the determination of chain direction.

4.4.1 *The extinction directions*

In a polarizing microscope, the light passing from the substage is plane polarized by passing through one of the devices already mentioned. In all modern microscopes this is a polaroid, a flat sheet of a chain polymer in which the chains lie parallel to each other and so constituted that one of the two vibrations passing through it, when light is incident on its lower surface, is absorbed. This plate is the *polarizer*. A second identical plate — the *analyzer* — is inserted in the body tube and one or both of the plates may be rotated about the optic axis of the microscope and the angular position read to 0.1°. Suppose — as is common — that the analyzer is the plate whose angular azimuth is measurable. As this plate is turned, keeping the polarizer fixed, the intensity of the light passing through the combination will vary. It will in principle fall to zero when the directions of allowed vibration in the two plates

lie at right angles. The polaroids are then said to be crossed. The light intensity is usually not quite zero because in neither polaroid is the unwanted vibration completely absorbed and for other reasons which will be taken up later (p. 94). It is, however, very low even when the incident intensity is high. Suppose that a thin transparent ribbon containing parallel aggregates of parallel molecular chains – say a single lamella in the wall of a plant cell – is then placed on the stage between the polarizer and the analyzer. In general the lamella will appear bright (while the background still, of course, is dark) for the following reasons.

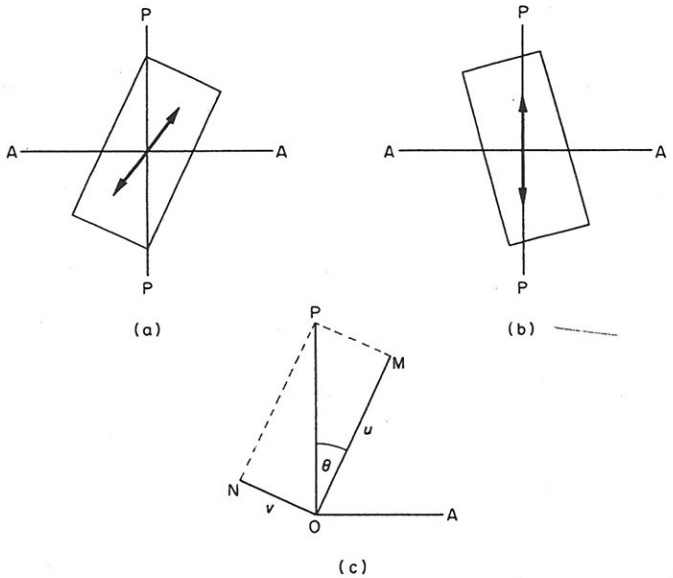

Fig. 4.8 (a), (b) PP and AA are the planes of vibration in the polarizer and analyzer respectively. The rectangle represents a cell wall, the arrow marking the direction of the constituent cellulose chains. (c) the optical situation represented in (a).

Looking down the microscope, let PP (Fig. 4.8) be the direction of vibration in the polarizer and AA that in the analyzer. In the general case the chain direction will lie at an angle θ to PP which is neither 0° nor 90° (Fig. 4.8a). The vibration PP is therefore resolved in the wall into two vibrations u and v (Fig. 4.8c) parallel and perpendicular to chain direction. Immediately upon entering

the wall these vibrations are in phase. Since, however, they are propagated through the wall with different velocities and therefore different refractive indices, they are in general no longer in phase upon leaving the wall. They cannot then reconstitute the original vibration. We shall need later on to consider the nature of the vibration which they do combine to reproduce, but all that we need to note now is that it is not PP. Now PP is the *only* vibration which has no component along AA. Hence this new vibration must yield a component along AA and the specimen must be bright. In the special case, however, when the chain direction lies parallel to PP, the original vibration passes through unchanged and is extinguished by AA (Fig. 4.8b). The specimen is then as dark as the field – it is said to be in an *extinction position*. Since the specimen will also be dark when the chain direction lies parallel to AA (since PP again passes through unchanged) it will be seen that there are four extinction positions per revolution as the stage is turned. In two of these the chains lie parallel to PP, the refractive index of the specimen is high, and the position is called the *major extinction position* (or the *slow direction* since the velocity of transmission is low). The other two are accordingly the *minor extinction position* (or *fast direction*), a term which it is not in practice often necessary to use. The directions of the crystal axes can therefore be determined but, since visually all the extinction positions are identical, it is impossible to distinguish the major position from the minor and hence to determine chain direction. By the use of an accessory device, however, this can be done quite simply in a matter of seconds, though an understanding of how it is done takes a little longer to explain.

4.4.2 *The major extinction position (m.e.p.)*

Consider the specimen, thickness d, viewed edgeways (Fig. 4.9) with monochromatic light, wavelength λ, incident upon the face at L. Two vibrations are propagated from L to M, with velocities c_γ and c_α and therefore wavelengths λ_γ and λ_α (since $\nu\lambda = c$ and ν is constant). Let λ_γ represent the vibration parallel to chain length and therefore correspond to the m.e.p. The numbers of wavelengths of each kind in distance d are d/λ_γ and d/λ_α. There is therefore in d a difference in the number of wavelengths amounting to $d(1/\lambda_\gamma - 1/\lambda_\alpha)$ and this is why the two vibrations

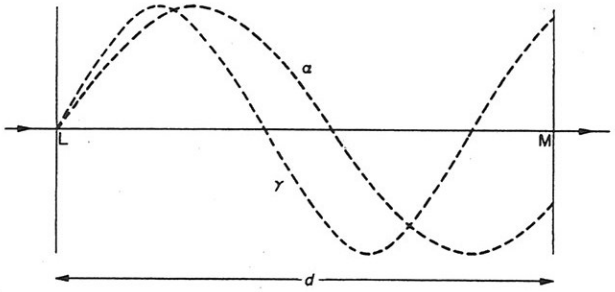

Fig. 4.9 For explanation, see text.

leave the specimen out of phase. Multiplication of this distance by λ_0 (the wavelength of the same light in air) gives the difference between the two paths, in the same units as d, as

$$p = d(\lambda_0/\lambda_\gamma - \lambda_0/\lambda_\alpha)$$
$$= (n_\gamma - n_\alpha)d$$

since $n = \lambda_0/\lambda_{(\text{medium})}$.
This is called the *path difference*. It corresponds to a *phase difference* (p. 71) equal to $2\pi p/\lambda$.
We can now assess in a more formal way the intensity of the light passing from the crystal in Fig. 4.8c. Let us represent the vibration PP as

$$s = a \sin \omega t$$

where a is the amplitude OP.
Then on entering the crystal this is resolved into two vibrations of amplitude u and v, represented therefore by

$$u = a \cos\theta \sin \omega t$$

$$\text{and } v = a \sin\theta \sin \omega t$$

On leaving the crystal each vibration has lagged behind the equivalent vibration *in vacuo* by, say, ϕ_u and ϕ_v where $(\phi_u - \phi_v) = \delta$, the phase difference. No rigour is lost by inserting δ in one of the vibrations instead of ϕ_u and ϕ_v in each vibration separately. Correspondingly, on leaving the wall, the vibrations have become, remembering that u is the m.e.p.,

$$u = a \cos\theta \sin(\omega t - \delta) \qquad 4.8a$$
$$v = a \sin\theta \sin \omega t \qquad 4.8b$$

These will combine to give a new vibration, the nature of which will be examined later. For the moment we maintain the equivalent position of keeping them separate and considering the sum of the resultant of each along AA. This is

$$s' = a \cos\theta \sin\theta \sin(\omega t - \delta) - a \sin\theta \cos\theta \sin \omega t$$

and must correspond to a single vibration of the form

$$s' = A \sin(\omega t + \Phi) \qquad 4.9$$

By equating terms in $\sin \omega t$ in Equations 4.8 and 4.9, repeating for terms in $\cos \omega t$ and squaring and adding the two expressions, we find

$$A^2 = \frac{a^2}{2} \sin^2 2\theta (1 - \cos\delta) \qquad 4.10$$

We note that A^2 is proportional to the light intensity. Clearly $A^2 = 0$ when $\theta = 0$, $\pi/2$, π, $3\pi/2$ or 2π and the specimen is extinguished four times per revolution. The intensity is also zero, irrespective of the value of θ, if $\cos\delta = 1$, i.e. $\delta = 0$, 2π, 4π, etc. and therefore $p = \lambda$, 2λ etc. This can also be derived from Fig. 4.9 since if the path difference is a whole number of wavelengths the two vibrations are in step on leaving the crystal as they were on entering it; they therefore re-form the original vibration *PP*.

Suppose, therefore, that the birefringent object under examination is a narrow wedge placed with one of the sloping sides on the stage of the microscope. Suppose that this is examined in blue light, $\lambda = 0.43\ \mu$m. Then at the apex of the wedge $\delta = 0$ and the intensity is zero. As the point of observation passes along the wedge the illumination increases and then decreases to zero at $\delta = 2\pi (p = 0.43\ \mu\text{m})$ and then increases much as in Fig. 4.10. The same behaviour occurs in yellow light ($\lambda = 0.56\ \mu$m) and red light ($\lambda = 0.7\ \mu$m) except that the second zero occurs further along the wedge (Fig. 4.10). If, therefore, all three wavelengths are presented together, the wedge will present various shades of grey up to a distance from the apex at which the path difference is about $0.2\ \mu$m (A, Fig. 4.10) because the intensity of all three radiations is increasing. Beyond this, the wedge will begin to appear coloured as the intensity of the blue component falls sharply and of the yellow component slowly, while the intensity of the red component is still increasing. At point B, path difference $0.43\ \mu$m, it will take on a brown to orange tinge. Similarly at C, path difference $0.56\ \mu$m,

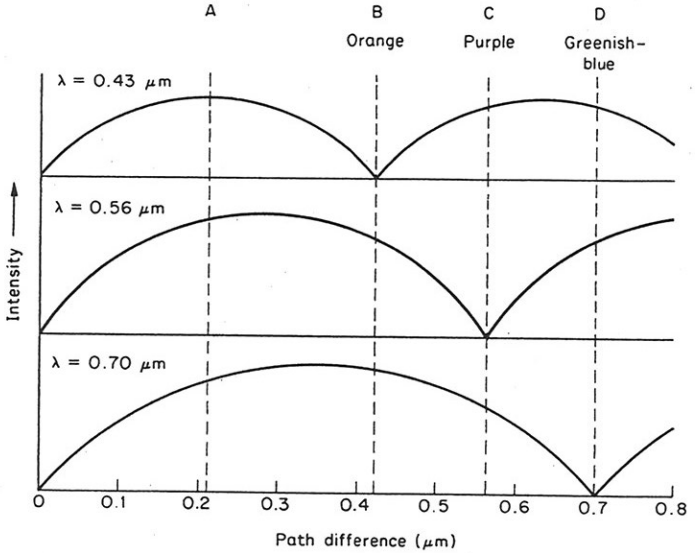

Fig. 4.10 The relative intensity of light emitted from a crystal between crossed polaroids as a function of path difference, for each of three wavelengths.

it will be purple and at D, path difference 0.7 μm, it will appear greenish-blue.

If the spectrum of wavelengths covered is now broadened to cover the whole visible region, i.e. if the wedge is observed in white light, clearly a very similar change of colour with path difference will be found, in a regular series. This is called Newton's series because the colour sequence is that found in the well-known Newton's rings phenomenon. The series is given in Table 4.1 both for crossed polaroids and parallel polaroids. Since the light corresponding to any wavelength is extinguished not only when $p = \lambda$ but also when $p = 2\lambda, 3\lambda$, etc., the colour sequence roughly repeats itself at intervals of $p = \lambda$. The sequences are therefore divided into orders. The point at which p is equal to the wavelength for green light ($p = 0.589\,\mu$m) is arbitrarily taken as the end of the first order colours; similarly $p = 1.178$, $p = 1.767$ marks the end of the second and third orders, and so forth.

These colour sequences have two major consequences. Firstly, a subjective estimate of the colour of a birefringent object gives a rough measure of the path difference. If, for instance, the colour is Red of the first order (Red I) (methods for determination of the

TABLE 4.1

The first two orders of Newton's colour scale (modified from Quincke)

Path difference (nm) (λ = 589 nm)	Order	Colour between crossed Nicols	Colour between parallel Nicols
0	I	Black	Bright white
40		Iron-grey	White
97		Lavender-grey	Yellowish-white
158		Greyish-white	Brownish-white
218		Clearer grey	Brownish-yellow
234		Greenish-white	Brown
259		Almost pure white	Light red
275		Pale straw-yellow	Dark reddish-brown
306		Light yellow	Indigo
332		Bright yellow	Blue
430		Brownish-yellow	Greyish-blue
505		Reddish-orange	Bluish-green
536		Red	Pale green
551		Deep red	Yellowish-green
565		Purple	Lighter green
575		Violet	Greenish-yellow
589		Indigo	Golden-yellow
664	II	Sky blue	Orange
728		Greenish-blue	Brownish-orange
747		Green	Light carmine
826		Lighter green	Purplish-red
843		Yellowish-green	Violet-purple
866		Greenish-yellow	Violet
910		Pure yellow	Indigo
948		Orange	Dark blue
998		Bright orange-red	Greenish-blue
1101		Dark violet-red	Green
1128		Light bluish-violet	Yellowish-green
1151		Indigo	Impure yellow

1 nm = 10^{-7} cm

order will be found on p. 92), then the path difference p is about 0.54 μm; if the specimen thickness d is 10 μm then, since $(n_\gamma - n_\alpha)d = p$, $(n_\gamma - n_\alpha)$ is 0.054 with a possible error which should not be greater than ±0.003. Of more importance, the rapid change in colour for a relatively small change in p (e.g. a change from red at 0.536 μm through purple and indigo to blue at 0.664)

a test plate can be used to determine the m.e.p. of any specimen, as follows.

Test plates are available, (e.g. of cleaved mica) which give any desired first or early second order colour between crossed polaroids; Red I and Violet I are common, the latter being known as the *sensitive tint plate*. The m.e.p. is known (by an independent method described in p. 87) and marked on the plate mount. The plate is inserted in the microscope between the objective and the analyzer in a slot which in modern microscopes is rotatable about the optic axis (Fig. 4.11a). It is so positioned that the m.e.p. lies at 45° to the planes of vibration in the polaroids and runs from bottom left to top right in the field of view (Fig. 4.11b). This is done by extinguishing the plate and then rotating it through 45° in the correct direction. The field will now appear, say, violet. A crystalline specimen placed on the stage and viewed through the

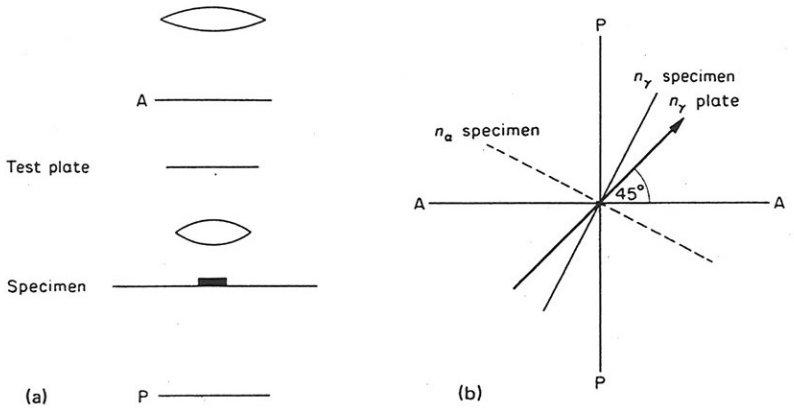

Fig. 4.11 (a) The point of insertion of a test plate in relation to the specimen, the polarizer, P, and the analyzer, A, in a polarizing microscope. (b) The corresponding optical diagram.

microscope will generally appear some other colour. If the m.e.p. lies is the position shown by a full line in Fig. 4.11b then, since it lies at less than 45° from the m.e.p. of the plate, the path differences are additive and the colour of specimen plus plate will be higher in Newton's series than that of the plate alone. Biological specimens mostly are of low path difference (in the range of the low first order colours in Table 4.1). The *addition* colour will be

therefore fairly close to violet, in the blue-green range. The specimen therefore appears green against a violet background. When, on the other hand, the stage is rotated so that the m.e.p. lies along the dotted line of Fig. 4.11b, the specimen shows a subtraction colour, say yellow. In the intermediate position when the m.e.p. is parallel to PP, the specimen has no effect on the light and therefore appears precisely the colour of the field. The position of the m.e.p. can now be determined.

Consider, for example, a tracheid or fibre of a higher plant over part of which one wall has been cut away so that the remaining single wall ABCD, Fig. 4.12, is available for examination. Suppose the m.e.p. lies along LM making an angle θ with the side wall BD. The position at which LM is parallel to PP, Fig. 4.11b, can be detected since the specimen will be precisely the same colour as

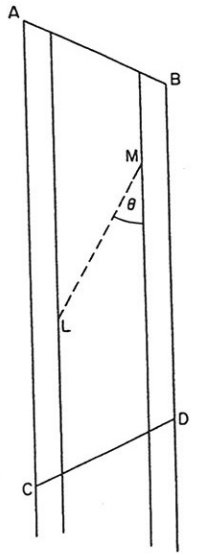

Fig. 4.12 Diagrammatic representation of a tracheid with one wall removed (above CD); LM represents the m.e.p. of the (lower) single wall.

the field. If the stage is now rotated clockwise through a few degrees the specimen colour will become an *addition* colour, say green. This verifies that the m.e.p. was parallel to PP, not AA. If the specimen shows a subtraction colour, say yellow, then the stage must be rotated through 90°. The method is therefore to begin by

setting the stage so that the specimen is extinguished, i.e. the same colour as the field, but goes into addition colour on clockwise rotation. This extinction position is achieved with much higher accuracy than it can be when the field is dark because the eye is much more sensitive to colour differences than it is to intensity differences at low light intensity. The angular position of the stage, θ_1, is noted. The analyzer is then removed from the light path and the stage rotated until the side BD lies parallel to PP (marked by a cross-wire in the eyepiece) and the position of the stage again noted, θ_0. Clearly $(\theta_1 - \theta_0) = \theta$. Each of θ_0 and θ_1 must be determined several times until agreement between successive readings is better than $\pm 0.5°$. Even then the eye may be mismatching slightly the colour of the specimen and that of the plate and it is always advisable to turn the stage through 90° to obtain a match when LM, Fig. 4.12, lies parallel to AA, Fig. 4.11. The angular distance between the two matching positions should be $90° \pm 0.5°$. If this is not the case the whole series of observations must be repeated. With practice, θ may be determined in as little as 30 seconds.

4.4.3 *Determination of refractive indices and birefringence*

We are now in a position to consider the determination of $(n_\gamma - n_\alpha)$. This can be done in a straightforward way by determining n_γ and n_α separately by a method which is simple to explain but tedious to carry out. Alternatively, and usually of more use, the birefringence $(n_\gamma - n_\alpha)$ may be determined within a few seconds by a method which requires lengthy explanation. We consider the direct method first and exemplify it by considering the refractive indices of the wall of a fibre.

In principle the method used for objects of microscopical size is a very simple one. It involves nothing more than finding a liquid medium in which there is no bending of the rays of light at the edge of the fibre, so that the fibre becomes almost invisible. It never does in practice become completely invisible for a number of reasons into which we need not go at the moment. Since the refractive index varies with the wavelength of the light used, it is customary to use monochromatic radiation given by a sodium vapour lamp, i.e. to use the sodium D line. The method can be tedious, but if a set of liquids is prepared beforehand differing in refractive index by, say, 0.01, and a sufficient quantity of material

in an adequate condition is at hand, then results come more quickly than might be imagined.

As a guide to the choice of the correct liquid a phenomenon first described by Becke and called the Becke line is employed. If the boundary between two media is observed under a microscope then a line of light is visible along the boundary if the refractive indices of the media are different. On raising the microscope objective, this line of light moves into the medium of higher refractive index. It is, therefore, a matter of a moment to decide whether the immersion liquid bathing a fibre has an index lower or higher than that of the fibre and thus to obtain a choice for the next liquid to be tried. The method, then, is briefly this. The fibre is mounted in a suitable medium of known refractive index on the rotating stage of a polarizing microscope and is set with the m.e.p. parallel to the direction of vibration of the light issuing from the polarizer. The analyzer is then moved out of the light path. Observation of the Becke line will show whether the refractive index of the medium is too high or too low. If it is too high, then a liquid of a lower index can be tried until the refractive index of the fibre is 'bracketed'; when by progressively narrowing the upper and lower limits, an increasingly close approximation to the refractive index of the fibre can be made. With care and under appropriate conditions, the refractive index can thus be determined to the third place of decimals. To obtain the necessary gradation in refractive indices it is necessary to use a mixture of liquids and a number of liquids are available. A very useful combination is α-monobromnaphthalene and liquid paraffin which fulfils the requirement that neither component shall swell the fibre (see below) and each shall have about equal volatility so that the refractive index of any mixture shall not change appreciably during the observation.

This determines the value of n_γ. n_α can be similarly determined with the appropriate orientation of the specimen.

Although, however, this technique presents no great difficulties the precise interpretation is not straightforward, on account of the physical and chemical heterogeneity of cell walls. The solid material of the wall consists of a family of polysaccharides and often other compounds such as lignin, varying from the completely amorphous to the truly crystalline; and there are 'void' spaces normally filled with water or an aqueous solution, some of which vary in size with water content. A prior decision has therefore

always to be made, in the light of the problem under investigation, as to the component whose refractive index is required, and how best to achieve the end in view. Consideration of these matters will be postponed, however, until we have before us the necessary details of wall architecture. Some, though not all, of these uncertainties, are avoided in determination of refractive index difference, the birefringence. The method here is to determine the path difference of a specimen and the specimen thickness in two separate operations. The path difference is normally low, in the range of 4 nm to 0.5 μm, so that the compensators used to determine path differences in inorganic crystals and petrological materials are too insensitive. There are, however, two compensators available, the de Sénarmont compensator and the Brace-Koehler or Elliptical compensator, effective in two ranges, which can give precise determinations of these low birefringences. To understand how these operate it is necessary to enquire into the form of the light vibration after it has passed out from the specimen into the body tube of the microscope.

(a) *de Sénarmont compensator*

Taking first the de Sénarmont compensator, the two linear vibrations just before leaving the specimen are as given in Equations 4.8a and 4.8b. With this, as with all compensators, the specimen is set so that $\theta = 45°$. The two vibrations are then

$$u = a/\sqrt{2} \sin(\omega t - \delta) \qquad 4.11a$$

$$v = a/\sqrt{2} \sin \omega t \qquad 4.11b$$

along the directions *ou* and *ov* (Fig. 4.13). These correspond to a single vibration figure which is the locus of points such as L (Fig. 4.13) in a curve referred to axes *ou* and *ov*. It is convenient to refer this curve to axes OA and OP. Equations 4.11 are therefore rewritten by substituting

$$x = (v - u)/\sqrt{2}$$

$$y = (v + u)/\sqrt{2}$$

giving

$$x = a(\sin \omega t - \sin(\omega t - \delta))/2$$

$$y = a(\sin \omega t + \sin(\omega t - \delta))/2$$

or,

$$x = a \cos(\omega t - \delta/2) \sin \delta/2 \qquad 4.12a$$

$$y = a \sin(\omega t - \delta/2) \cos \delta/2 \qquad 4.12b$$

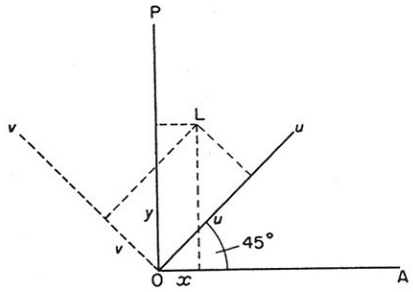

Fig. 4.13 For explanation, see text

Squaring and adding, we have

$$x^2/(a^2 \sin^2 \delta/2) + y^2/(a^2 \cos^2 \delta/2) = 1, \qquad 4.13$$

an ellipse with axes parallel to OP and OA and with axial ratio $\tan \delta/2$ (Fig. 4.14). This is the form of vibration required. The original plane vibration on passing through the crystal is always transformed into an elliptical vibration invariably of this form. Determination of δ is therefore resolved into the determination of the slope of a diagonal of the rectangle circumscribing the ellipse (Fig. 4.14).

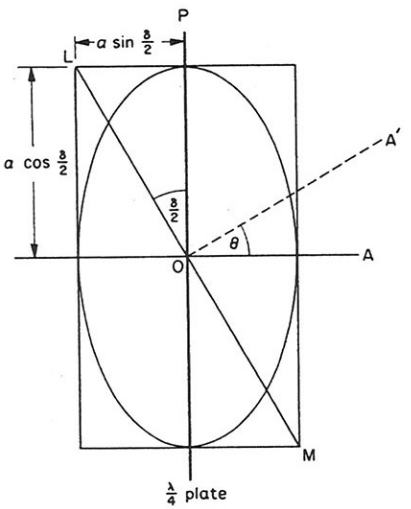

Fig. 4.14 For explanation, see text.

In devising a means to do this we note that Equations 4.12 may be rewritten

$$x = (a \sin \delta/2) \sin(\omega t - \delta/2 - \pi/2) \qquad 4.14a$$

$$y = (a \cos \delta/2) \sin(\omega t - \delta/2) \qquad 4.14b$$

These are the two vibrations parallel to axes OP and OA into which the elliptic vibration can be resolved; whatever the value of δ they themselves always differ in phase by $\pi/2$. If now we impose a phase lag on vibration y (|| OP) of $\pi/2$ by inserting in the light path a crystal plate with phase difference $\pi/2$ (and therefore path difference of $\lambda/4$ so that this is called a *quarter wave plate*) with its m.e.p. parallel to OP, then this in effect removes the $\pi/2$ phase difference in Equations 4.14. They then become

$$x = (a \sin \delta/2) \sin(\omega t - \delta/2)$$

$$y = (a \cos \delta/2) \sin(\omega t - \delta/2)$$

i.e. $$x/y = \tan \delta/2$$

and the vibration is the straight line LM (Fig. 4.14).
This may be extinguished by rotating the analyzer through an angle θ to bring its plane of vibration perpendicular to LM, where

$$\theta = \delta/2$$

and the phase difference is determined. The path difference p is then $\delta\lambda/2\pi$.

It is perhaps more instructive – as well as being useful when we come to consider interference microscopy – to examine this compensator in a different way. Equation 4.13 shows that for a quarter wave plate ($\delta = \pi/2$)

$$x^2 + y^2 = a^2$$

and the ellipse becomes a circle. Any plane vibration incident upon a quarter wave plate with the direction of vibration lying at 45° to the crystal axes becomes transformed on passing through the crystal into a circular vibration. This may also be seen pictorially as follows. Let PP Fig. 4.15 represent a plane vibration incident normally on a crystal at 45° to the crystal axes *lf*, *ci*. The two vibrations in the crystal then correspond to *lf* and *ci*. We need to define path lengths along *lf* and *ci* of equal time interval. This may be done (cp. Fig. 4.2) by constructing a circle centre *o*, radius *ol* (= *oc*) and marking out equal lengths of arc along the

circumference of this circle ($a - l$ in Fig. 4.15). Perpendiculars dropped on *lf* and *ci* from points *a*, *b*, *c*... then mark out the required lengths. When the vibration PP enters the crystal, corresponding points in the two vibrations will lie at *l* and *i*. If the crystal has a path difference of $\lambda/4$ then, on leaving the crystal, when a point in vibration *lf* is at *l*, the equivalent point on *ci* will

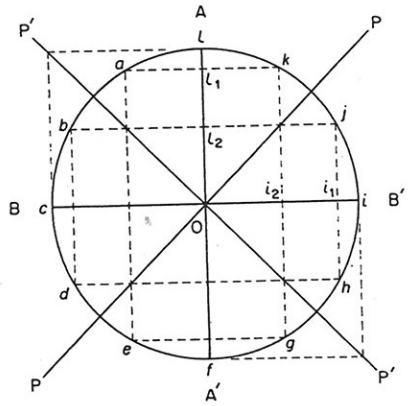

Fig. 4.15 For explanation, see text.

be at *o* and moving to the right; the net displacement is therefore at *l*. By the time the point has moved from *l* to l_1 the point at *o* has moved to i_2; the net displacement is at *k*. Similarly, by the time the point on *lf* has reached l_2, the point on *li* has reached i_1, and the net displacement is at *j*; and so forth. The resultant vibration is therefore the circle *lkj....a*, rotating clockwise. Similarly, a plane vibration P'P' on passing through the crystal becomes an identical circular vibration but rotating anticlockwise. This leads to a simple geometric explanation of the de Sénarmont compensator.

PP' (Fig. 4.16) represents the original vibration from the polarizer and AA', BB' the vibration directions in the specimen (at 45° to PP'), LL' and QQ' represent the vibration directions in the superposed quarter wave plate. The vibrations AA' and BB' become transformed into two circular vibrations of diameter AA' rotating in opposite directions. If these two vibrations are in phase, then when the point in one circle is at A, the point on the other must be at B' and two circular vibrations compound to give a plane vibration LL'. This is extinguished by the analyzer. If the vibration

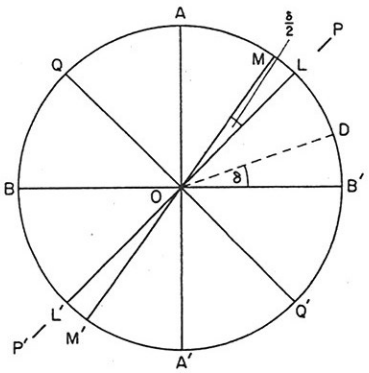

Fig. 4.16 **For explanation, see text.**

BB′ lags behind AA′ by a phase difference, δ, then when the point corresponding to AA′ lies at A that corresponding to BB′ lies at D, where ∠ DOB′ is δ. The two circles therefore collapse into a linear vibration MM′ making an angle of δ/2 with PP′. It is therefore necessary to turn the analyzer through an angle of δ/2 to extinguish the specimen.

The use of the compensator should now be clear. A λ/4 plate is inserted in the body tube of the microscope and extinguished between crossed polaroids (accuracy ±0.50°). The specimen is inserted, extinguished, and rotated through 45° to maximum brightness. The analyzer is then rotated until the specimen is extinguished and its position read; the angular displacement is δ/2. Alternatively and better, the specimen may be rotated 90° and the analyzer again rotated to specimen extinction, when the angular rotation from one extinction to the other is δ. It should be noted that a rotation of 180° from the crossed position corresponds to a path difference of λ and that the measurement yields only the fraction of a wavelength; i.e. if the path difference is 3.4λ the measurement gives only 0.4λ; the whole number of wavelengths which must be added may be determined by a wedge compensator. Most biological objects which can be examined microscopically will, however, show a path difference less than λ. The compensator gives satisfactory results in white light but for highest accuracy the wavelength must be used for which the λ/4 plate is calibrated. It is not especially accurate for path differences of λ/20 or lower and for path differences below this the following compensator comes into use.

(b) *The elliptic or Brace-Koehler compensator*

The principle of this compensator follows from the discussion above leading to Equation 4.13. We begin with Equations 4.8a and b referring to Fig. 4.8c. Eliminating t from these and, for a reason which will be seen below, writing ϕ_0 instead of δ, we have

$$\frac{u^2}{a^2\cos^2\theta} + \frac{y^2}{a^2\sin^2\theta} - \frac{2uv}{a^2\sin\theta\cos\theta}\cos\phi_0 = \sin^2\phi_0$$

This is an elliptic vibration referred to axes u and v, inscribed in a rectangle of sides $2a\cos\theta$ and $2a\sin\theta$ (Fig. 4.17) and describes the form of the vibration passing out from a crystal in the general case. As before, when ϕ_0 is small this is an ellipse with axes closely parallel to PP and AA. To determine the form of this ellipse transform to co-ordinates axes PP and AA by using

$$x = u\sin\theta - v\cos\theta \qquad 4.15a$$

$$y = u\cos\theta + v\sin\theta \qquad 4.15b$$

Substituting from Equation 4.15a into Equation 4.8a and Equation 4.15b into Equation 4.8b, and taking the case for small values of ϕ_0 so that $\cos\phi_0 = 1$ and $\sin\phi_0 = \phi_0$, we have

$$x = (a/2)\sin 2\theta\cos\omega t.\phi_0$$

$$y = a\sin\omega t - a\sin^2\theta\cos\omega t.\phi_0$$

The amplitude of x is therefore $(a/2)\sin 2\theta.\phi_0$ and of y is a. The ratio of these, $\frac{1}{2}\sin 2\theta.\phi_0$, gives the ratio of the axes of the ellipse. When, therefore, a test plate, phase difference ϕ_0, is placed in the

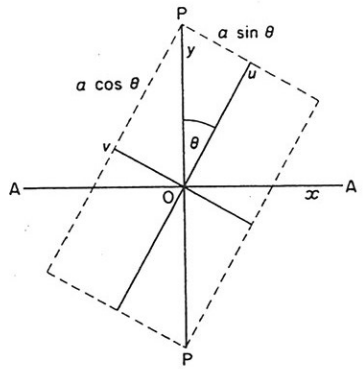

Fig. 4.17 **For explanation, see text.**

microscope with the m.e.p. lying at an angle θ to PP, the vibration passing from the plate is an ellipse, with axes closely parallel to PP and AA and with axial ratio $\frac{1}{2}\sin 2\theta.\phi_0$. We have already seen (Equation 4.13) that for a specimen placed with its m.e.p. at 45° to PP the resultant vibration is an ellipse with axes parallel to PP and AA and axial ratio $\tan \delta/2$ ($= \delta/2$ for δ small). If this is the same ellipse as the ellipse from the test plate, but rotating in the opposite direction, then the specimen is extinguished and

$$\delta = -\phi \sin 2\theta$$

In using this compensator, therefore, the specimen is set at 45°. The compensator, consisting of a plate with a path difference of say $\lambda/30$ and rotatable in its plane about the optic axis, is inserted and rotated until the field is extinguished. The angle θ is the angular movement of the compensator plate then required to extinguish the specimen.

In measuring such small path differences it is necessary to reduce reflection depolarization by blooming the objective lenses, to use the best polaroids available and to employ high light intensity.

4.4.4 *The interpretation of the m.e.p. and the path difference*

The determinations of the m.e.p. and the path difference in a biological specimen are therefore straightforward; their interpretation is, however, usually not so. Let us consider first the m.e.p. Only under the circumstance that, in the wall specimen under observation, the lengths of the submicroscopic crystallites – now known to be the cores of the microfibrils, a term we shall now use – lie in the plane of the wall, the wall is homogeneous as regards microfibril direction and the optical character of the microfibrils is known, does the m.e.p. in any sense determine the run of the microfibrils. If these conditions obtain then the m.e.p. corresponds to the mean molecular chain direction and therefore to the mean microfibril direction in cellulosic walls, or to the perpendicular to this direction in walls containing microfibrils within which the constituent chains run in slow helices as in xylan walls (Frei and Preston, 1964) (p. 255). Even then it should be remembered that the polarization microscope is highly sensitive to orientation; a small proportion of oriented microfibrils in a mass

which is randomly scattered will give rise to a detectable m.e.p. Correspondingly, a slight departure from absolute randomness, detectable only through severe precautions in the electron microscope, can readily be detected under the polarizing microscope [as in *Bryopsis* (Frei and Preston, 1964)]. The degree of order can then roughly be defined only by determination of the refractive indices or the birefringence. The necessary discussion on this matter must, however, be postponed until the general structure of the wall has been presented.

A real specimen may depart from the above ideal either in that the microfibrils do not lie in the plane normal to the optic axis of the microscope or in that the microfibril orientation is not homogeneous throughout the specimen thickness. We examine the related complexities in turn.

(a) *Microfibrils tilted to plane of surface*

The effect of microfibril tilt can best be understood through a specific example. Consider a rectangular piece of a single wall lamella cut from the secondary wall of a fibre or tracheid (Fig. 4.18). Within this the microfibrils lie parallel to the surface of the lamella but usually tilted to cell length. Suppose the microfibrils lie perfectly parallel to each other. Observation in direction *A* yields an m.e.p. which correctly defines the microfibril direction. Equally observations in directions *B* and *C* do not; the correct orientation may nevertheless still be deduced in the following way.

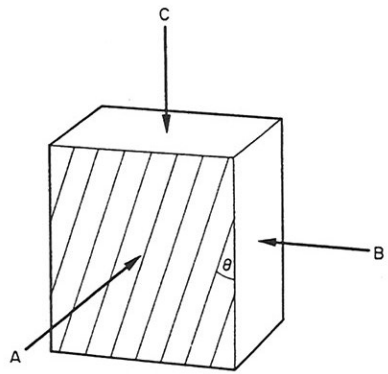

Fig. 4.18 A segment of a cell wall, the striped area being one surface of the wall; the stripes are parallel to the m.e.p.

It should first be recalled that for such a set of parallel molecular chains the refractive index for light vibration parallel to chain direction is greater than that for any other vibration direction. Equally, since the molecular chains of cellulose consist of a series of rings which, although somewhat puckered, are still rather flat and lie in the same plane, then for light propagated *along* the chains, the refractive index should be greater for light vibrating *parallel* to the plane of the rings than *perpendicular* to this plane. In this sense, cellulose should have three characteristic refractive indices, n_γ, n_β and n_α respectively. There are in the literature vague statements that this is true for cellulose but it is difficult to see how the relevant evidence can validly be obtained. It is usually taken that for cellulose $n_\beta = n_\alpha$ so that only two refractive indices need be considered. This places cellulose in the class of crystals which, for a reason given below, is called *uniaxial*.

As we have seen, n_γ and n_α can be determined directly only for light propagated through the wall lamella normal to microfibril length (or, for n_α only, parallel to this length). In light propagated in some other direction refractive indices intermediate between n_γ and n_α are yielded, the value depending on the direction of propagation. It is found that all these refractive indices can be correlated in the following way. Suppose an ellipsoid of rotation is constructed (Fig. 4.19) with half the major axis equal in length to n_γ and half the minor axis equal to n_α and the ellipsoid – the *index ellipsoid* – oriented in the wall with the major axis parallel to chain direction. Then for light propagated in any general direction *MO* (Fig. 4.19) a plane vibration will be resolved into two vibrations parallel to the axes of the ellipse formed by the intersection of the plane normal to the direction of propagation with the ellipsoid, with refractive indices equal in magnitude to the lengths of the major and minor axes, respectively, of the ellipse. Notice that the smaller refractive index is always n_α. The other refractive index, n_γ', may be calculated. The method may be exemplified through the common case in which a transverse section of a cell is under examination, i.e. the direction of propagation is *A* (Fig. 4.19).

The geometry of the situation is set out in Fig. 4.20 representing a plane section through Fig. 4.19 parallel to the lamella surface; the refractive index required is n_γ^{L} (L signifying that the refractive index is the major refractive index in the transverse plane). Then

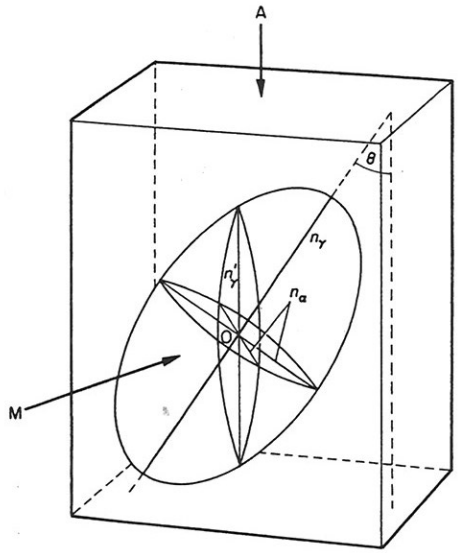

Fig. 4.19 The index ellipsoid.

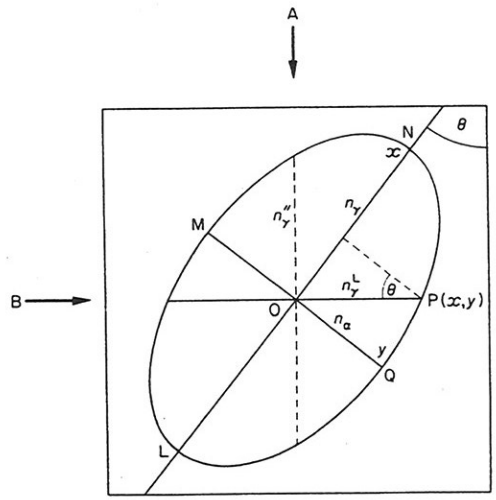

Fig. 4.20 The trace of the index ellipsoid on a plane parallel to wall surface, cell axis ↕.

calling the n_γ direction the x axis and the n_α direction the y axis the point P has coordinates x, y related by

$$\frac{x^2}{n_\gamma^2} + \frac{y^2}{n_\alpha^2} = 1,$$

the equation of the ellipse LMNP. This may be rewritten

$$\frac{(n_\gamma^{\mathrm{L}})^2 \sin^2\theta}{n_\gamma^2} + \frac{(n_\gamma^{\mathrm{L}})^2 \cos^2\theta}{n_\alpha^2} = 1 \qquad 4.16$$

whence $(n_\gamma^{\mathrm{L}})^2 = (n_\gamma^2 n_\alpha^2)/(n_\gamma^2 - (n_\gamma^2 - n_\alpha^2)\sin^2\theta)$

What is usually measured (and all that can be measured for a wall lamella lying inside a wall) is $(n_\gamma^{\mathrm{L}} - n_\alpha)$, from the path difference. n_α may usually be taken as 1.53. If n_γ is known, θ may be calculated; equally if θ is already known, n_γ may be calculated.

If neither n_γ nor θ is known then the refractive indices must be measured also in some other direction, e.g. in longitudinal section B (Fig. 4.20). The appropriate major refractive index is then n_γ'' for which

$$\frac{(n_\gamma'')^2 \cos^2\theta}{n_\gamma^2} + \frac{(n_\gamma'')^2 \sin^2\theta}{n_\alpha^2} = 1 \qquad 4.17$$

Equations 4.16 and 4.17 may be combined to give:

$$n_\gamma^2 = (n_\gamma'')^2 n_\alpha^2 (n_\gamma^{\mathrm{L}})^2 / [(n_\gamma'')^2 n_\alpha^2 + n_\alpha^2 (n_\gamma^{\mathrm{L}})^2 - (n_\gamma'')^2 (n_\gamma^{\mathrm{L}})^2];$$

$$\sin^2\theta = [(n_\gamma^{\mathrm{L}})^2 (n_\gamma'')^2 - n_\alpha^2 (n_\gamma'')^2] / [(2n_\gamma'')^2 (n_\gamma^{\mathrm{L}})^2 - n_\alpha^2 (n_\gamma'')^2 - (n_\gamma^{\mathrm{L}})^2 n_\alpha^2]$$

Since n_γ'' and n_γ^{L} are known and n_α is known (1.53) or measurable, n_γ and θ may be calculated. The structure of bamboo fibres was worked out in this way (Preston and Singh, 1951).

It should be noted that, for light propagated along the direction of the major axis of the index ellipsoid, the locus of intersection of the ellipsoid with the plane normal to this direction is a circle so that $n_\gamma = n_\alpha$. Viewed in this direction the microfibril array is isotropic; the direction is a unique direction, the optic axis, and this is why crystals of this kind are called uniaxial.

(b) *Superposed wall lamellae differing in m.e.p.*

The other complexity – lack of homogeneity in the wall – commonly takes the form that the wall consists of a number of thin

superposed lamellae different in chain orientation. Examples occur with *Valonia* (Preston and Astbury, 1937), the Cladophorales (Astbury and Preston, 1940; Frei and Preston, 1961) and in tracheids and fibres (Preston, 1947; Preston and Singh, 1951) and many other cell types. Indeed, any whole single cell always poses this problem. Microfibrils are normally tilted to the cell axis and therefore run helically round the cell; the microfibrils of front and back walls are therefore crossed (Fig. 4.21) and examination of the central regions A of the cell (but obviously not of the side wall B) presents the problem of two superposed crystal plates with crossed axes. In this case the problem is trivial since one wall can be (and must be) cut away to leave the other free for examination. It is nevertheless of profit to consider this problem first. The appropriate diagram is as in Fig. 4.22.

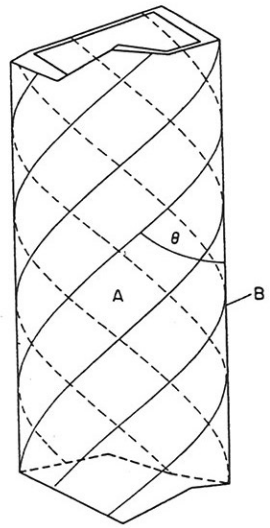

Fig. 4.21 Diagrammatic representation of the run of the m.e.p. in a whole cell. B, side wall in optical section; A, two superposed walls with crossed m.e.p.'s.

The analytical process already used for single crystal plates is first followed. The vibration along PP ($s = a \sin \omega t$) is resolved along ou_1 and ov_1 as before. Now, however, each is resolved in turn along ou_2 and ov_2 and the component of these vibrations along AA calculated. The procedure is then as before; the calculation

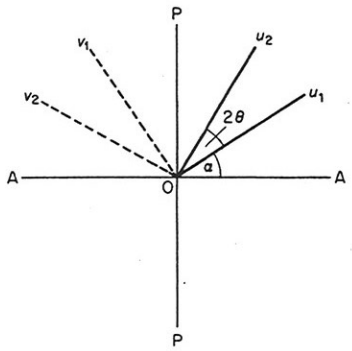

Fig. 4.22 **For explanation, see text.**

is more tedious but leads straightforwardly to

$$
\begin{aligned}
I/I_0 &= -\sin 2\alpha \cos 2(2\theta + \alpha) \sin 4\theta \sin^2(\phi_1/2) \\
&\quad + \cos 2\alpha \sin 2(2\theta + \alpha) \sin 4\theta \sin^2 \phi_2/2 \\
&\quad + \sin 2\alpha \sin 2(2\theta + \alpha) \cos^2 2\theta \sin^2 [(\phi_1 + \phi_2)/2] \\
&\quad - \sin 2\alpha \sin 2(2\theta + \alpha) \sin^2 2\theta \sin^2 [(\phi_2 - \phi_1)/2] \\
&= (\sin 2\alpha \sin(\phi_1/2))^2 + (\sin 2(2\theta + \alpha) \sin(\phi_2/2))^2 \\
&\quad + 2 \sin 2\alpha \sin 2(2\theta + \alpha) \sin(\phi_1/2) \sin(\phi_2/2) \cos \phi'
\end{aligned}
$$

where I and I_0 represent respectively the intensity of light passing through the analyzer and of the incident beam, ϕ_1 and ϕ_2 are the two phase differences and ϕ' represents the third side of a spherical triangle as in Fig. 4.23.

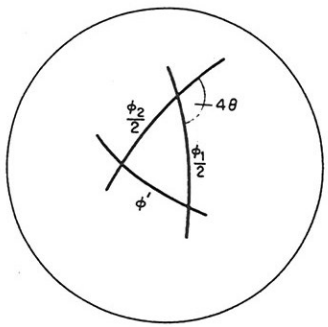

Fig. 4.23 **For explanation, see text.**

The second version of this equation is of the form $(a^2 + b^2 + 2ab \cos \phi')$. The specimen can be extinguished at some value of α only if (1) $a = b$ and $\cos \phi' = -1$ or (2) $a = -b$ and $\cos \phi' = 1$ or (3) $a = b = 0$. If ϕ_1, ϕ_2 and θ are given none of these can be true; indeed, if 2θ is not zero or $\pi/2$ or π, extinction may be achieved only if the path differences ϕ_1 and ϕ_2 are multiples of λ (i.e. $a = b = 0$). As the specimen is rotated on the stage, therefore, its intensity does not fall to zero at the 'extinction positions' but to a minimum less than zero. For a typical cell $\phi_1 = \phi_2$ and the minimum of intensity then occurs when $\alpha = 90° - \theta$ or $-\theta$, i.e. when cell length lies either parallel or perpendicular to PP. If $2\theta < 45°$ the m.e.p. lies parallel to cell length; if $2\theta > 45°$ and $< 90°$ it lies perpendicular to cell length.

The double wall of a whole cell does not therefore behave like a single, homogeneous wall (note that the side walls B, Fig. 4.21, do so behave and therefore extinguish).

The physical reason for the lack of extinction may best be seen through the use of a model – the Poincaré sphere – which has the advantage that a multi-lamella problem with a single wall can also be dealt with in an elegant way such as would be unacceptably tedious by the analytical method used above. The tedious algebra is built into the model and automatically dealt with by the construction. The properties of the sphere will be given without the proof which involves mathematical considerations too complex to handle here; the proof may be found in Poincaré (1889–92) or Pockels (1906) (see also Ramachandran and Ramaseshan 1961; Harsthorne and Stuart 1970). The sphere may be represented as a globe with poles, N, O (Fig. 4.24), an equator ABPXY, lines of latitude EGF and of longitude NGPO. The significance of these lines is that they represent at every point two directions in real space normal to the direction of light waves travelling toward an observer outside the sphere. All points on the equator represent *linear vibrations* whose directions vary on passing round the equator such that diametrically opposite points (e.g. P, L) represent vibrations at right angles. We adopt the convention that on passing anticlockwise round the equator (viewed from above) the vibration also rotates anticlockwise. Clearly to pass through two points such as P and X with a difference in vibration direction α we need to pass round the sphere through an angular distance 2α. All points on the sphere away from the equator except the poles correspond

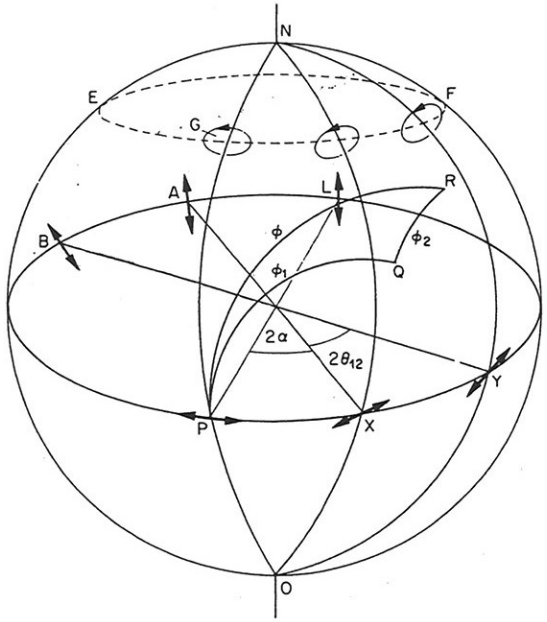

Fig. 4.24(a) The Poincaré sphere.

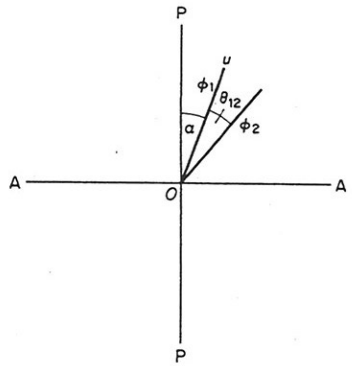

Fig. 4.24(b) For explanation, see text.

to elliptic vibrations. Lines of latitude such as EG represent ellipses rotating in the same direction, anticlockwise above the equator and clockwise below, with equal axial ratio. Lines of longitude represent ellipses of equal orientation but decreasing in ellipticity from the equator (at which they collapse into linear vibrations)

to the poles which represent circular vibrations. Consider now the problem illustrated in Fig. 4.24b.

Let point P, Fig. 4.24a, on the equator, represent the incident plane vibration PP, Fig. 4.24b. In order to plot the effect of the passage of this vibration through the plate of phase difference ϕ_1, move around the equator from P to X through an angle 2α. The plane vibration at X lies at an angle α to that at P and represents ou, one of the vibrations in the first crystal plate; the diametrically opposite point A represents the other vibration. Now rotate the equator circle round the axis XA through an angle ϕ_1, bringing P along a small circle to Q. Q represents precisely the elliptical vibration passing out from the first plate. To determine the effect on this of the second crystal, move further along the equator from X to Y, through an angle $2\theta_{12}$, and rotate about the equatorial diameter YB through an angle ϕ_2, bringing Q to R. R represents the effect of the passage of the plane vibration PP through both plates. Clearly the passage from P to R may be achieved directly by rotation about a single diameter, but this is not an equatorial diameter. Since rotation only about an equatorial diameter corresponds to passage through a simple birefringence plate, the path difference ϕ equivalent to the arc PR does not represent such a plate only. What is does represent may be seen by noting that rotation about any diameter of the sphere is equivalent to rotation about an equatorial diameter plus a rotation about a polar diameter. Rotation about an equatorial diameter represents a component of the plate combination which is itself a simple birefringent plate. Rotation about a polar diameter clearly corresponds to a second component which is a circularly polarizing plate. It is this second component, exercising its effect whatever the orientation of the crossed crystal plates to the plane of vibration of the polarizer, which ensures that the crossed plates are never extinguished.

Rotation about a third, fourth... equatorial diameter corresponds to passage of the light vibrations through a third, fourth, etc. crystal plate so that any number of crossed plates can be dealt with by the Poincaré sphere. Note that if the resulting polygon is closed, the combination represents only a circularly polarizing plate.

The construction required therefore is very simple. For the plates indicated in Fig. 4.25b, one begins by drawing an arc, length ϕ_1 (D_1D_2) (Fig. 4.25a) corresponding to the Plate 1. A second arc D_2D_3 is constructed, length ϕ_2, making an external angle of $2\theta_{12}$

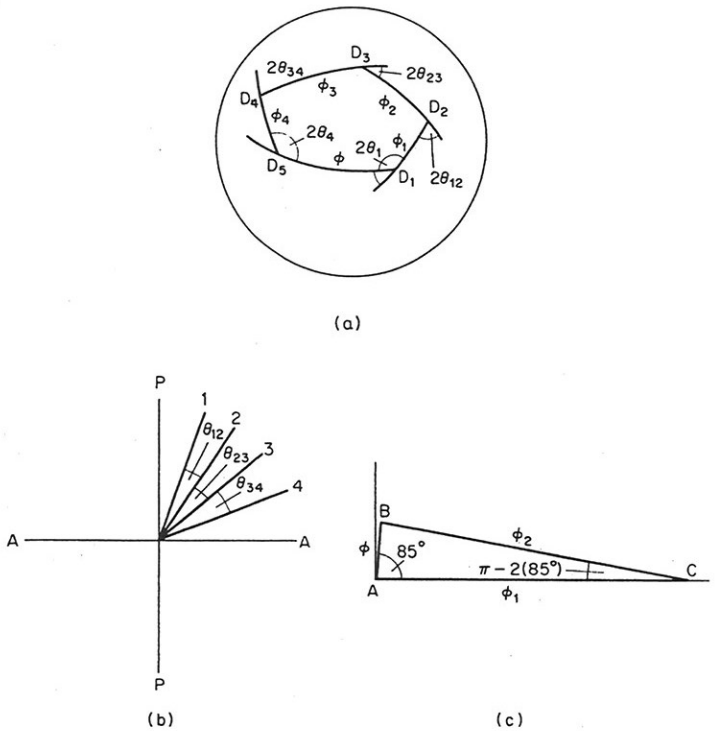

Fig. 4.25 For explanation, see text.

with D_1D_2. Similarly for D_3D_4 and D_4D_5. The arc required to close the polygon gives ϕ, the phase difference of the corresponding birefringent plate and θ_1 gives the angle between the m.e.p. of this plate and that of plate 1 (the internal angle this time, because formally the phase difference ϕ is that required to close the polygon and therefore with m.e.p. lying at right angles to that of the resultant of the plate combination).

Since the resulting polygon is drawn on a sphere,

$$2\theta_{12} + 2\theta_{23} + 2\theta_{34} + 2\theta_{41} = 2\pi - \beta$$

β is an index of the strength of the circularly polarizing component.

In most instances in biology the ϕs are all small. This means that in effect the sphere is of large diameter, the polygon is plane, and the circularly polarizing component disappears; the polygon can be drawn on flat paper. The order in which the individual plates

are taken is then immaterial (it is not so in the general case). An illustrative example may serve to show how the method may help in otherwise recalcitrant problems (a second example will be found on p. 295). The wall of a cell of *Chaetomorpha melagonium* (p. 203) 15 μm thick consists of a number of superposed cellulosic lamellae alternating in chain direction through an angle of 85° given by optically visible striations on the wall. These lamellae are very thin (say about 20 nm) and their phase differences and *a fortiori* that of the whole wall, is small. Since therefore the order in which the lamellae are taken is irrelevant, the wall may be taken as two layers each 7.5μ thick. The path difference of the whole wall is 0.035 μm and the m.e.p. bisects the acute angle between the striations. The question is, does this harmonize with the presence of cellulose as the only crystalline material? Set out line AB, (Fig. 4.25c), length 0.035 units making an angle of 85° (twice the angle between one striation direction and the m.e.p.) with the abcissa taken as one striation direction. AB represents in magnitude and direction the path difference of the whole wall. Draw a line from B making an angle of $2(\pi/2 - 85°) = 10°$ to the abcissa, intersecting the abcissa at C. BC and AC are the path differences of each layer separately. These are naturally identical and each is found, either graphically or by calculation, equal to 0.202 units. The path difference of each is therefore 0.202 μm and the birefringence is (0.202/7.5) = 0.027. Since the wall thickness contains only 45 per cent cellulose, the birefringence of the constituent cellulose should be 0.06 = (0.027/0.45) which is correct. The path difference of the whole wall therefore harmonizes with its cellulosic nature.

4.4.5 *Birefringence and its interpretation*

It will be clear that birefringence is derived by dividing the path difference by specimen thickness. The latter must be determined, of course, under conditions as closely like those used with the former. With a cylindrical cell it can often be assumed that the wall is uniform so that the side walls (measurable by an eyepiece micrometer) may be used. Similarly, with care sections may be stood on edge and the thickness measured in a similar way. The best method, though time-consuming, is to use an interference microscope for direct determination at the point at which the path

difference has been determined (p. 117).

The significance to be attached to birefringence of a wall lamella depends upon the conditions under which it is determined, in terms of the heterogeneity of the lamella. To a first approximation crystalline components in the form of long thin rods – the microfibrils – may be taken as immersed in a matrix of non-cellulosic polysaccharides (p. 188) and other substances which are optically amorphous and possess voids of submicroscopic dimensions (p. 375). In nature the lamella is saturated with water and therefore swollen. Determination of the refractive indices n_γ and n_α separately demands the use of organic embedding liquids. There must therefore, be no excess water on the specimens and the liquids must be such as not to extract water. The method is in any case not easy. Birefringence $(n_\gamma - n_\alpha)$ may, however, be determined without ambiguity and may be interpreted (see below).

If the birefringence of the intact wall is required, drying by any method which induces shrinkage has at least two undesirable consequences. Firstly, the mere act of shrinking is liable to change the orientation of the microfibrils, and therefore the birefringence, by an amount which is unascertainable. Secondly, the change in volume and increase in refractive index of the non-crystalline component relative to the crystalline component (by the withdrawal of water from the non-crystalline component only) automatically changes the birefringence. This involves the principle that an array of isotropic parallel rods of submicroscopic diameter immersed in a liquid will appear optically anisotropic if the refractive index of the liquid differs from that of the rods. The theory of such a system was worked out by Wiener (1912) who showed that the birefringence of such a body is

$$n_\gamma^2 - n_\alpha^2 = \frac{\delta_1\delta_2(n_1^2 - n_2^2)^2}{(\delta_1 + 1)n_2^2 + \delta_2 n_1^2}$$

Where δ_1 and δ_2 are the relative volumes of the rods and the liquid respectively $(\delta_1 + \delta_2 = 1)$, n_1 is the refractive index of the rods and n_2 that of the liquid, n_γ is the refractive index for light vibrating parallel to the rods and propagated in a direction perpendicular to their lengths and n_α is the refractive index for light vibrating at right angles to their lengths. The system is clearly uniaxial and the birefringence is referred to as *form birefringence*. For present purposes we note only that the birefringence varies

with δ_1 or δ_2. In a wet cell wall containing parallel microfibrils, n_1 may be taken as 1.5 and n_2 as 1.45 at least. Taking $\delta_1 = \delta_2 = 0.5$, then $(n_\gamma - n_\alpha) = 0.001$. On drying this may drop no lower than zero (if e.g. n_1 then equals n_2). The total change in birefringence is then 0.001 and this may be ignored if the microfibrils are cellulose with an intrinsic birefringence of about 0.06. With an unknown wall, however, it is always best to check the presence of form birefringence by determining the birefringence in a number of liquids of different refractive indices which penetrate the wall but do not swell or shrink it.

As far as the individual refractive indices n_γ and n_α of the wall are concerned, it is usually safer to determine these in dried specimens and for purposes of comparison it has become standard practice to make the determinations on material dried over P_2O_5 and to accept some small error due to re-orientation. Even then the refractive indices cannot of course be accepted as the refractive index of e.g. cellulose in a cellulosic wall. We need to add here the complication that the wall is not a two-phase system as assumed above but a multiphase system consisting at least of (a) cellulose (b) non-cellulosic polysaccharides, some chains of which are parallel [and parallel to the microfibrils (p. 165)], (c) randomly arranged polysaccharide chains and other non-crystalline components such as lignin, (d) an aqueous solution in voids. Denoting the relative volumes by f and the refractive indices by n and assuming that the wall behaves as a liquid (as it does in this context to a fair approximation) then

$$n_{\gamma_{\text{wall}}} = f_a n_{\gamma a} + f_a n_{\gamma b} + f_c n_c + f_d n_d$$

$$n_{\alpha_{\text{wall}}} = f_a n_{\alpha a} + f_a n_{\alpha b} + f_c n_c + f_d n_d$$

$n_{\gamma a}$ and $n_{\alpha a}$ (which are usually what are required) may be determined only if the other refractive indices and the relative volumes are known. Note that

$$n_{\gamma_{\text{wall}}} - n_{\alpha_{\text{wall}}} = (n_{\gamma a} - n_{\alpha a}) f_a + (n_{\gamma b} - n_{\alpha b}) f_b$$

The second term on the right is difficult to assess and it is customary to assume $n_{\gamma a} = n_{\gamma b}$ and $n_{\alpha a} = n_{\alpha b}$, to add $f_a + f_b$ $(= f)$ and write

$$n_{\gamma_{\text{wall}}} - n_{\alpha_{\text{wall}}} = (n_{\gamma a} - n_{\alpha a}) f$$

f is taken as the volume of polysaccharide, relative to the total

volume, after extractable polysaccharide and other material have been removed. $n_{\gamma a} - n_{\alpha a}$, which refers to cellulose (or other skeletal polysaccharide) may then be calculated.

4.5 Interference microscopy

Interference microscopy is dealt with here only in broad principle and only in so far as it forms a useful adjunct in cell wall studies as, for instance, in determining wall thickness for birefringence determination, and in checking the condition of material for electron microscopy. Further details will be found in a number of text books (e.g. Françon, 1961; Ross, 1967; Oster and Pallister, 1956; Barer and Mellor, 1955), and detailed methods of use are readily available in the manuals referring to individual commercial microscopes. Phase contrast microscopy will be considered as an imperfect interference microscope.

Most biological material in thin section is transparent, that is to say that light vibrations passing through it are not reduced in amplitude or therefore in intensity. The vibrations are nevertheless affected by passage through the material since the various parts of the section – or a cell – have different refractive indices which are all normally different from the refractive index of the embedding medium. This induces differences in phase which are related to refractive indices. Consider a thin sheet of cell wall, thickness t and with mean refractive n_s surrounded by a liquid of refractive index n_o. Then the optical thicknesses of wall and liquid, for light propagated in a direction normal to the surface are $n_s t$ and $n_o t$ respectively. The light transmitted through the wall then lags behind that transmitted through the liquid by a path difference $\Delta = [(n_s - n_o)t]$, equivalent to a phase difference of $2\pi\Delta/\lambda$ for monochromatic light of wavelength λ. The eye cannot detect differences in phase so that the contrast with such a *phase object* – so-called in distinction from an absorbing object called an *amplitude object* – is zero. The purpose of interference microscopy is to convert such small phase differences into amplitude differences, so that contrast is achieved and, more relevant to the discussions here, to use this contrast in determining Δ and hence both the refractive indices and the thickness. This is achieved in different ways in the phase contrast microscope and in interference microscopes so that these must be

considered separately. We take phase contrast microscopes first.

For the cell wall plate mentioned above, let the vibration o, Fig. 4.26, represent the light transmitted by the surrounding liquid and s that transmitted by the wall with a lag of Δ. In principle o has been converted to s by passage through the specimen. This conversion could be achieved in another way. Consider a third vibration d, Fig. 4.26, of the same wavelength as o and s but with a smaller amplitude, a' and lagging behind o by a path length $\lambda/4$. Then even by inspection it can be seen that d and o can be added to give s. This can be shown formally in the following simple way.

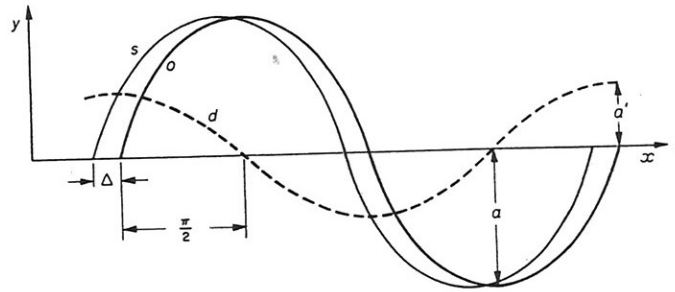

Fig. 4.26 For explanation, see text.

Vibrations s and o are of the form

$$y = a \sin 2\pi x/\lambda$$

Hence

$$a' = a \sin 2\pi\Delta/\lambda$$
$$= a 2\pi\Delta/\lambda$$

since the phase difference is small.
Vibrations o and d may therefore be written:

$$y = a \sin 2\pi x/\lambda$$
$$y' = a 2\pi\Delta/\lambda \sin(2\pi x/\lambda - \pi/2)$$
$$= a 2\pi\Delta/\lambda \cos 2\pi x/\lambda$$

Adding y and y' give a vibration

$$y'' = a \sin 2\pi x/\lambda + a 2\pi\Delta/\lambda \cos 2\pi x/\lambda \quad 4.18$$
$$= A \sin(2\pi x/\lambda + \phi) \quad 4.19$$

since this must be a sine wave, where ϕ is a new phase difference. Equating terms in $\sin 2\pi x/\lambda$ and $\cos 2\pi x/\lambda$ between Equations 4.18 and 4.19 and squaring and adding gives

$$A^2 = a^2(1 + (2\pi\Delta/\lambda)^2)$$
$$= a^2,$$

and dividing gives

$$\tan\phi = 2\pi\Delta/\lambda$$

i.e.

$$\phi = 2\pi\Delta/\lambda$$

since $2\pi\Delta/\lambda$ is small.
The resultant vibration is therefore

$$y'' = a \sin 2\pi/\lambda(x - \Delta)$$

which is vibration s.
Without for the moment considering the physical nature of d, suppose now a second path difference of $\pi/2$ is imposed on vibration d (by passing it through a plate of optical thickness $\lambda/4$ for example). Then d becomes

$$y' = a2\pi\Delta/\lambda \sin 2\pi x/\lambda$$

whereas o remains

$$y = a \sin 2\pi x/\lambda$$

These are now in opposition and may be directly subtracted giving

$$A^2 = a^2(1 - 2\pi\Delta/\lambda)^2$$
$$= a^2(1 - 4\pi\Delta/\lambda) \qquad 4.20$$

where A is the resultant amplitude. This converts a phase difference into an amplitude difference with the object darker than the field. Note that if the vibration d is *advanced* through $\lambda/4$ then $A^2 = a^2(1 + 4\pi\Delta/\lambda)$ and the specimen is brighter than the field. Both conditions can be realized.

It is therefore necessary to consider the physical nature of vibration d so that this relation may be used. d is clearly the sum of the rays diffracted by the specimen, and the proposition is that the vibrations transmitted by the object are the vector sum of the vibrations transmitted through the background and the vibrations diffracted by the object. Since the paths of these two vibrations are not the same, then clearly in principle the diffracted rays may be passed through a $\lambda/4$ plate to give the condition leading to

Equation 4.20, so that the specimen is darker (or brighter) than the field.

The principle is illustrated in Fig. 4.27 for a specimen consisting of a line grating and the practical situation in a phase contrast microscope is shown in Fig. 4.28. The direct light passing through

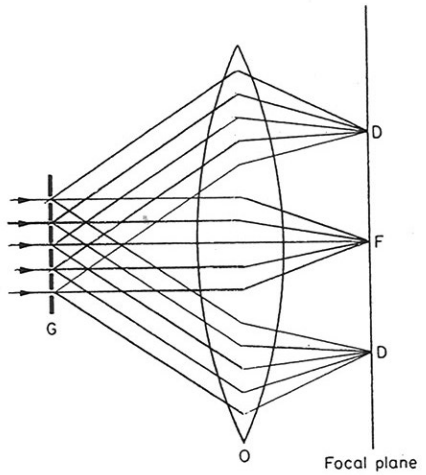

Fig. 4.27 The diffraction image of a line grating G at the back focal plane of the objective, O.

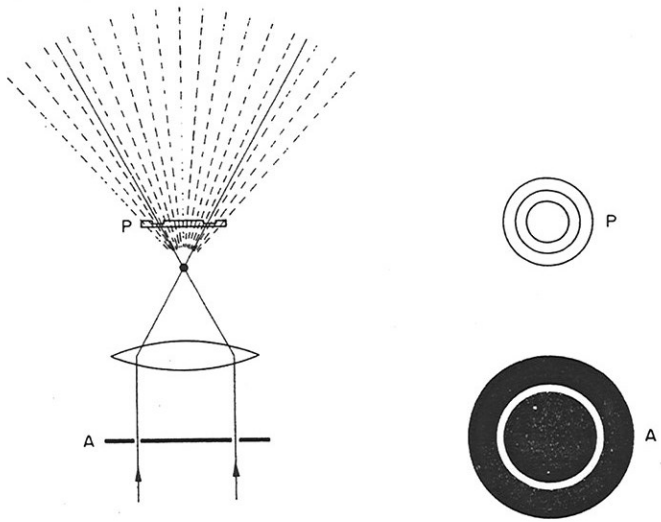

Fig. 4.28 The principle of construction of a phase contrast microscope.

the microscope is confined to a hollow cone and this light passes through an annulus in a plate P (Fig. 4.28), above the object, of depth equivalent.to $\lambda/4$. The diffracted light mostly passes through the rest of plate P, inducing a phase lag of $\pi/2$. In view of the discrepancy in intensity between the incident and diffracted beams, the annulus is usually part-silvered in order to reduce the intensity of the direct beam. Most manufacturers provide phase plates with 70–90 per cent absorption and these have some advantages as will be seen below; however, they have also some drawbacks.

Equation 4.20 refers only to conditions under which Δ is small compared with λ, and under these conditions the intensity varies linearly with Δ. This is no longer true for higher values of Δ as can be seen from a (very simplified) vectorial treatment of the situation. Let the incident vibrations be represented by a line OM (Fig. 4.29) of length equal to the amplitude a and with a phase determined by the direction of OM. On passing through the specimen, OM is changed in phase by an amount ϕ and may be

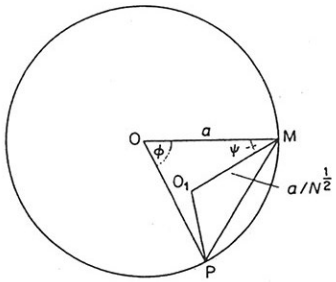

Fig. 4.29 **Simplified vector diagram for phase contrast microscopy.**

represented as OP, making an angle ϕ with OM. The line MP is the vectorial sum of OM and OP and is therefore equivalent in amplitude and phase to the diffracted beam. When ϕ is small, the angle OMP (the phase) is almost 90° as we have seen. MP and OM are together equivalent to OP. In the microscope OM is reduced in intensity and changed in phase by an amount ψ. This can be represented by rotating MO about M through an angle ψ and reducing its length to $a/N^{\frac{1}{2}}$ (i.e. reducing the intensity by a factor N). O then moves to O_1 and the resultant intensity of the specimen is O_1P. This intensity can obviously be calculated from triangle O_1MP and it is clear that in the general case the relation between

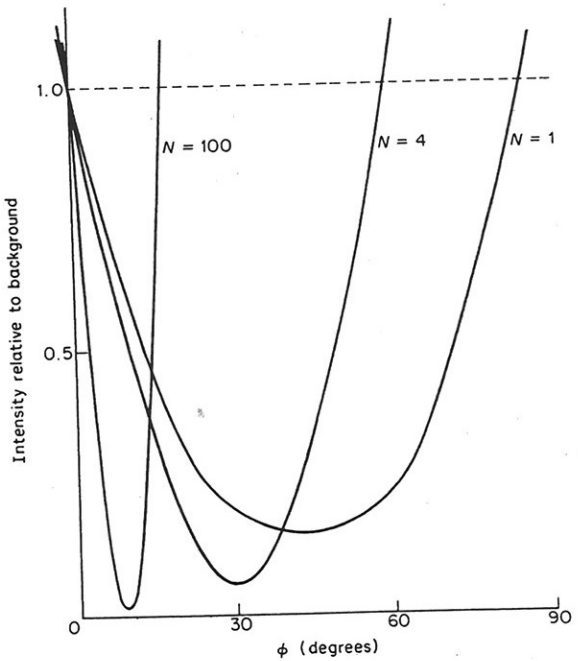

Fig. 4.30 **The relative intensity of light from objects of difference phase retardation in terms of the absorbancy of the wave plate annulus.**

phase and intensity is not linear. The corresponding relations for various values of N are presented in Fig. 4.30, because they present a dilemma of which users of microscopes with a fixed phase plate must be constantly aware.

A phase plate of high absorption gives high contrast for small phase changes but is completely insensitive to large phase changes. Unless this is realized, the appearance of a specimen may be misleading. On the other hand, a phase plate of lower absorption, while covering a wider range of phase, is not as sensitive at low phases as is the highly absorbing plate. The real dilemma is, however, that with any phase plate the intensity of the specimen is the same for two values of the phase and the observer cannot distinguish between these unless a second phase plate of different absorption is available.

Phase contrast microscopes have other disadvantages in addition, deriving from the circumstance that some of the diffracted light

passes through the annulus of the phase plate so that these microscopes are in effect only imperfect interference microscopes. This has two effects upon the image (Fig. 4.31). Firstly, the microscope is sensitive only to abrupt changes in phase and these are associated with a halo, bright for dark specimens and dark for bright specimens, which obscures edges and makes measurement of phase difficult. Secondly, specimens show what is known as the 'shading effect'; in this, an extended area of uniform refractive index which would be expected to be uniformly dark appears brighter in the centre than at the edges and can even appear brighter than the field. This effect is not normally noticeable with a cell containing numerous organelles but is marked when cell walls are observed in surface view, precluding any accurate measurements.

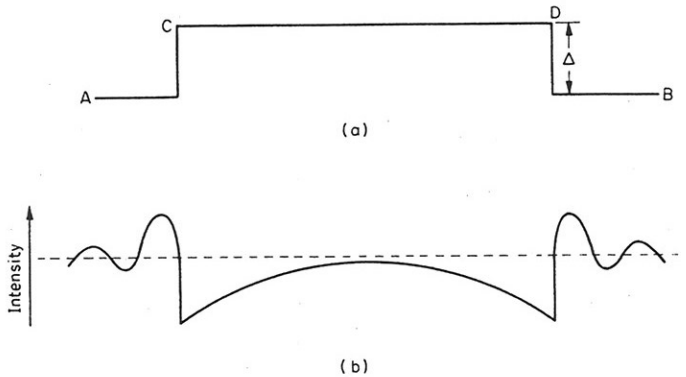

Fig. 4.31 (a) The path difference Δ between the wave front CD passing through an optical uniform object and the corresponding wave front in the medium. (b) The corresponding intensity distribution observed in a phase contrast microscope.

Nevertheless, phase contrast microscopes have certain clear advantages over the more perfect interference microscopes. They are simple to use and relatively cheap, perfectly adequate for checking the condition of material being processed for examination by other techniques such as electron microscopy. The image is more 'pleasing' than it is with interference microscopes. The microscope's insensitivity to moderate variation in phase imposes no demands with regard to variations in microscope slide thickness and objects of extended area can be observed.

Interference microscopes do not make use of the separation of the diffracted and direct beams. Instead, the incident beam is split into two so that two statistically coherent beams pass through the microscope and are brought together so that they interfere. Only one of these beams passes through the specimen so that the visible field consists of two overlying fields, one containing the background only and the other with the specimen superposed. The beams can be separated only by a small distance so that only small objects, or the edges of large objects, are displayed under conditions in which the phase is measurable.

The principle of this microscope may be understood from Fig. 4.32, analogous to Fig. 4.29. OM and OP are again the incident illumination and the illumination transmitted by the specimen. The second beam introduced into the microscope and passing through the background only is OO_1, differing in phase from OM by a

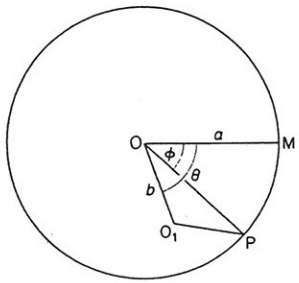

Fig. 4.32 Simplified vector diagram for interference microscopy.

variable phase angle θ and perhaps in amplitude. Again the vectorial addition of OO_1 and OP is O_1P and this gives the amplitude of the specimen beam. Again this amplitude depends on ϕ only, for any given value of θ. The situation expressed by Fig. 4.30 applies also here but is less serious since θ may be varied at will and ambiguity in the value of ϕ can be avoided.

ϕ may be determined in either of two ways. In the more sensitive approach the microscope is set, following the instruction in the manual, so that the phase difference of the empty field is constant over the whole field. The incident intensity of the specimen beam is then OM (Fig. 4.33), the transmitted intensity OP and the comparison beam intensity OO_1 (now made of the same amplitude as OM). As the phase θ is increased, O_1 moves round the circle MPV'.

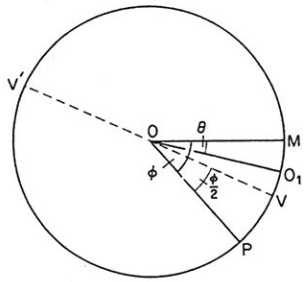

Fig. 4.33 For explanation, see text.

The background intensity is therefore always O_1M^2 and the specimen intensity O_1P^2. When $\theta = 0$, O_1 coincides with M and the specimen intensity is MP^2, i.e. the specimen is bright against a black background. As θ is increased up to $\phi/2$ the specimen darkens and the background lightens until at $\theta = \phi/2$, when O_1 is at V, a cross-over point occurs at which the specimen and background are of the same intensity and beyond which the specimen continues to darken. The position $\theta = \phi/2$ can be used as a sensitive measure of ϕ since θ is known. Note that there is a second match at V′ but this is very insensitive and can readily be distinguished from the match at V. When $\phi = \theta$, O_1 is at P and the specimen is black against a bright background. This position can also be used to determine ϕ.

If, on the other hand, the field is set to a constant gradient of phase difference, the field is covered by a series of equidistant fringes. The phase difference of a specimen can again be determined as in Fig. 4.34 but this is a much less accurate procedure, and is not to be recommended.

When white light is used the field, and the fringes, are coloured. A matching of colours then means a matching of phases and this proves useful in examining cell walls.

The more readily available interference microscopes are of one of two types. In one, the splitting of the incident beam into two is achieved by the Dyson method in which internal reflection in a narrow wedge below the specimen achieves the splitting and the two beams are recombined by reflection in a second identical wedge placed above the specimen. In the other the illumination is divided by passage through a thick crystal, separating the beam into two beams polarized at right-angles to each other. These are

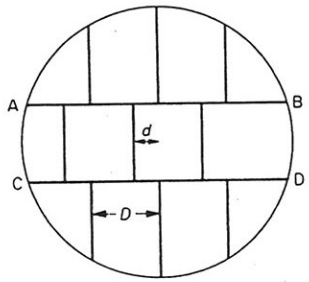

Fig. 4.34 A strip of material, ABCD, viewed in an interference microscope with a gradient of phase difference across the field. The fringes, spacing equivalent to one wavelength, are displaced in the object by a distance d, proportional to $\phi[\equiv(d/D)\lambda]$.

subsequently recombined in a second identical crystal after passing through a $\lambda/2$ crystal plate which turns the direction of each beam through a right angle. Since beams of light vibration at right-angles to each other cannot interfere, a $\lambda/4$ plate is inserted in the light path which converts the two plane polarized beams into two circularly polarized beams rotating in opposite directions (see p. 90), which then interfere.

The thickness of a cell wall may be determined in either of these microscopes, but care is needed with those using polarization-splitting since the light passing through the specimen plane is plane polarized; the object needs to be suitably oriented.

Since

$$\Delta = (n_s - n_o)t$$

and n_o is known and Δ measurable, t is known if n_s is known (this may be taken as the average of n_γ and n_α). If n_s is not known then two observations of Δ need to be made in media of different refractive index. Then

$$\Delta = (n_s - n_o)t$$

$$\Delta' = (n_s - n_o')t$$

where Δ' and n_o' are the second values. Hence

$$t = (\Delta' - \Delta)/(n_o - n_o')$$

whence n_s may be calculated.

Alternatively, if t is known, n_s may be calculated in one operation. This may be used to give a rough estimate of composition. If, for

instance, a wall has a relative volume of cellulose Σ and a relative volume of lignin $(1 - \Sigma)$, then

$$n_s = \Sigma n_c + (1 - \Sigma) n_e$$

where n_e is the refractive index of lignin (1.46). Hence Σ may be determined. Or, if a wall consists entirely of substances of refractive index n_w but there is a relative void volume Σ, then

$$n_s = (1 - \Sigma) n_w + \Sigma$$

Hence, taking n_w as 1.55, Σ may be calculated and hence the density, $(1 - \Sigma)_{\rho_c}$, where ρ_c is the density of cellulose.

CHAPTER 5

Structure determination – X-ray diffraction

It is now clear that the individual long molecular chains which for the most part constitute the cell walls of plants already show some order. The sugar residues in a homogeneous chain occur in regular sequence along the chain so that in most β-1,4-linked glucans, for instance, the glycosidic oxygen bridges occur regularly at intervals along the chain of 5.15 Å. All that is needed to specify the chain is the nature of the residue and the spacings of 5.15 Å. If a number of chains can be induced to lie parallel to each other then a higher degree of order is achieved whether or not the chains are spaced regularly the same distance apart. This higher degree of order can be detected, and to some extent quantified, by optical methods which were described in the last chapter. We now confine attention to the situation in which the chains lie not only parallel to each other but spaced regularly side by side, that is the situation in which the polysaccharide achieves full three-dimensional order. In all cell walls there is at least one polysaccharide which is synthesized in three-dimensional order and which therefore occurs in intact walls in a form open to examination by any method which can interpret the order. In the large bulk of cell walls this is cellulose and this particular polysaccharide will be taken as an example of the use of the most powerful tool available for the study of three-dimensional order – X-ray diffraction analysis. As already mentioned, it is now known that in some plants cellulose does not occur and its place is taken over by another polysaccharide, and equally it is known that many polysaccharides which do not occur naturally in three-dimensional order can be induced to take up this order by various extraction and precipitation methods; these will, however, be discussed in the appropriate place in ensuing chapters.